JOURNAL OF SPACECRAFT AND ROCKETS
Vol. 38, No. 6, November–December 2001

Integrated Aeropropulsive Computational Fluid Dynamics Methodology for the Hyper-X Flight Experiment

Charles E. Cockrell Jr.* and Walter C. Engelund†
NASA Langley Research Center, Hampton, Virginia 23681-2199
Robert D. Bittner,‡ Tom N. Jentink,§ and Arthur D. Dilley¶
FDC/NYMA, Inc., Hampton, Virginia 23681-2199
and
Abdelkader Frendi**
University of Alabama in Huntsville, Huntsville, Alabama 35899

Computational fluid dynamics tools have been used extensively in the analysis and development of the X-43A Hyper-X Research Vehicle. A significant element of this analysis is the prediction of integrated vehicle aeropropulsive performance, which includes an integration of aerodynamic and propulsion flowfields. The development of the Mach 7 X-43A required a preflight assessment of longitudinal and lateral-directional aeropropulsive characteristics near the target flight-test condition. The development of this preflight database was accomplished through extensive aerodynamic wind-tunnel testing and a combination of three-dimensional inviscid airframe calculations and cowl-to-tail scramjet cycle analyses to generate longitudinal performance increments between mission sequences. These increments were measured directly and validated through tests of the Hyper-X flight engine and vehicle flowpath simulator in the NASA Langley Research Center 8-Foot High Temperature Tunnel. Predictions were refined with tip-to-tail Navier–Stokes calculations, which also provided information on scramjet exhaust plume expansion in the aftbody region. A qualitative assessment of lateral-directional stability characteristics was made through a series of tip-to-tail inviscid calculations, including a simulation of the powered scramjet flight-test condition. Additional comparisons with wind-tunnel force and moment data as well as surface pressure measurements from the Hyper-X flight engine and vehicle flowpath simulator model and wind-tunnel testing were made to assess solution accuracy.

Nomenclature

C_A	=	axial force coefficient
$C_{l\beta}$	=	rolling moment derivative, /deg
C_M	=	pitching moment coefficient
C_N	=	normal force coefficient
$C_{n\beta}$	=	yawing moment derivative, /deg
C_p	=	pressure coefficient
$C_{y\beta}$	=	side force derivative, /deg
X, Y, Z	=	spatial coordinates, m
α	=	angle of attack, deg

Introduction

HYPERSONIC airbreathing vehicle configurations are characterized by highly integrated propulsion flowpath and airframe systems. Aerodynamic performance cannot be decoupled from engine performance and operability because the external forebody and nozzle surfaces are part of the engine flowpath. Therefore, a significant challenge in the development of this class of vehicle is an assessment of propulsion–airframe flowfield interactions and the determination of integrated aeropropulsive performance of candidate systems. Advanced experimental, analytical, and computational tools are being developed to aid in the design of configurations that exploit propulsion–airframe interactions to maximize performance and enhance stability and control characteristics. Presently, capabilities for testing complete engine flowpath–airframe configurations that model all of the pertinent interactions affecting integrated vehicle performance are limited in terms of scale and simulation of powered effects. Predictive methodologies, including computational fluid dynamics (CFD) and other analysis tools, must encompass a wide range of modeling capabilities to capture all of the relevant flow physics of the complete scramjet flowpath as well as the external airframe. This analysis is normally accomplished using a multilevel approach, increasing in complexity and fidelity as the design is matured. The preliminary analysis phase may employ different tools for the various flowpath components, which necessitates the development of force accounting systems appropriate for specific configurations. CFD is also a valuable tool used to interpret aerodynamic and propulsion ground-test data.

One objective of the Hyper-X program is to develop and mature the technologies required for hypersonic airbreathing flight.[1] Three flight tests of the Hyper-X Research Vehicle, or X-43A, are currently scheduled to obtain in-flight performance data on a scramjet-powered hypersonic configuration. The first two of these flight tests will be at Mach 7 test conditions with a third flight at Mach 10. The X-43A preflight database utilized CFD predictions to develop the basic longitudinal performance characteristics for the vehicle throughout the mission profile.[2] The accuracy of these predictions was assessed through comparisons with available ground- test data. Lateral-directional stability was also examined with inviscid CFD predictions. Computations were also used to address other aspects of vehicle performance and flight-test development, including boundary-layer trip design and assessment,

Presented as Paper 2000-4010 at the AIAA 18th Applied Aerodynamics Conference, Denver, CO, 14–17 August 2000; received 26 October 2000; accepted for publication 20 June 2001.

*Aerospace Engineer, Hypersonic Airbreathing Propulsion Branch, MS 168. Senior Member AIAA.

†Aerospace Engineer, Vehicle Analysis Branch, MS 365. Senior Member AIAA.

‡Section Supervisor, Hypersonic Numerical Applications Section, Hyper-X Program Office; currently Group Supervisor, Hypersonic Vehicle Analysis Group, Swales Aerospace, Inc., Hampton, VA 23681-2199.

§Research Engineer, Hyper-X Program Office; currently Research Engineer, Swales Aerospace, Inc., Hampton, VA 23681-2199.

¶Research Engineer, Hyper-X Program Office; currently Senior Systems Engineer, Aeromechanics Design Department, Raytheon Electronic Systems, 1151 E. Hermans Road, Tucson, AZ 85706.

**Associate Professor, Department of Mechanical and Aerospace Engineering.

thermal and structural loads, and scramjet flowpath component performance.

The Hyper-X program also represents the first opportunity to correlate analytical and CFD predictions with ground-test and flight-test data on an airframe-integrated scramjet configuration. Comparisons with ground and flight data will be used to further calibrate tools and physical models. Because the CFD and experimental test techniques used in the Hyper-X program represent the state of the art in hypersonic propulsion–airframe integration research, an examination of these methods also provides insight into future technology development needs for the next phase of hypersonic vehicle development.

This paper presents an overview of the methods used in the analysis and preflight database development for the Mach 7 X-43A vehicle. A discussion of CFD codes and other analysis tools is included with their respective capabilities and limitations. The appropriateness of various physical modeling approximations and their effect on performance predictions is discussed. The methodology for integration of tools for various flowpath components is discussed with limited results and comparisons to available ground-test data.

Mission Description and Analysis Requirements

The nominal Hyper-X Mach 7 flight trajectory is shown in Fig. 1. The flight profile begins with the captive carry flight of the Hyper-X Launch Vehicle (HXLV) under the wing of a B-52 aircraft. The HXLV consists of the X-43A mounted to the first stage of a Pegasus booster rocket with a vehicle-to-booster adapter. Following air launch of the HXLV from the B-52, the launch vehicle is boosted to the appropriate flight-test condition and, at burnout, the X-43A separates from the booster. Upon stabilization, the cowl door, which remains closed throughout the boost phase to block the inlet entrance and protect the internal engine components from high heat loads during boost, opens to establish flow through the engine. Following a few seconds of unpowered operation, hydrogen fuel is introduced, and the powered portion of the scramjet test is conducted, lasting approximately 7 s. A series of parameter identification (PID) maneuvers are then conducted, and the cowl door closes as the vehicle begins a controlled descent before mission termination, while conducting additional PID maneuvers to measure lower Mach number aerodynamic stability and control characteristics. This flight profile necessitates the analysis of three distinct mission phases: cowl-closed unpowered, cowl-open unpowered, and cowl-open powered. Much of the analysis for aeropropulsive performance is built on the prediction of force and moment increments between the various mission points. The term inlet-open increment is used to refer to the difference in force and moment quantities between the cowl-open unpowered and cowl-closed points and the term power-on increment is used to refer to the difference between the cowl-open powered and cowl-open unpowered phases of the flight.

A complete nose-to-tail analysis of the X-43A at the conditions of interest requires a wide range of flow modeling capabilities. A summary of the relevant flow physics and prediction requirements is shown in Fig. 2. At hypersonic Mach numbers, high-temperature gas effects become important. For the Mach 7 Hyper-X flight conditions, it is sufficient to model the external flowfield as a frozen mixture of thermally perfect gases, where thermodynamic quantities vary as a function of temperature using curve fits for the appropriate species. Composite species models may be used to approximate the composition of the scramjet exhaust products as a single thermally perfect species to reduce computational overhead. Surface pressure and skin-friction predictions are generally required on all external surfaces to resolve vehicle forces and moments and to provide structural loadings on vehicle components. Heat transfer predictions may also be required to assess thermal loads. This implies the need for appropriate turbulence models and knowledge of the boundary-layer state. Accurate computations of forebody flowfields, characterized by shocks, shock–boundary-layer interactions and potentially separated flow regions are required to compute mass

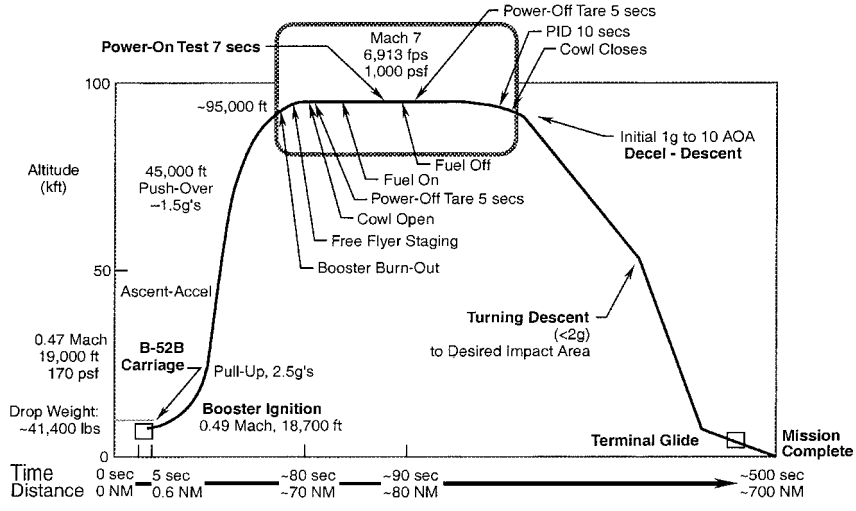

Fig. 1 Hyper-X Mach 7 flight trajectory.

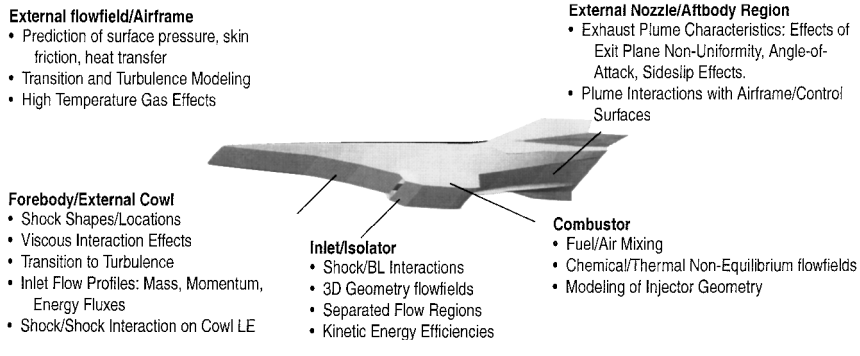

Fig. 2 X-43A flow physics and modeling requirements.

capture at the cowl lip station. The inlet flowfield is characterized by shock–boundary-layer interactions, flow separation in unfavorable pressure gradients, high leading-edge thermal loads, and corner flow regions. Accurate computation of the inlet region provides throat properties for evaluation of component performance. Computation of the combustor flowfield requires modeling fuel injection and complex mixing phenomena as well as finite-rate chemical reactions. Upstream pressure rise in the isolator also occurs due to heat addition in the combustor. Downstream of the combustor, the high-temperature scramjet exhaust flowfield must be modeled by approximating the species constituents of the combustion process. This powered exhaust plume expands in the aftbody region and may interact with vehicle aerodynamic or control surfaces, especially at deflected wing settings or when the vehicle is at nonzero angles of attack or sideslip.

The determination of integrated vehicle performance requires analysis of both internal and external flowfields with an appropriate accounting of the interactions between the two. Engine operability and performance has a direct impact on overall vehicle aerodynamic forces and moments. Axial force contributions from the flowpath have a direct impact on net thrust and acceleration. However, resolution of normal force and pitching moment is also important because vehicle trim characteristics affect trim drag penalties, which, in turn, affect system operability and performance. Therefore, contributions from both external aerodynamic and propulsion flowpath components must be considered. The objective of the computations performed on the X-43 was to develop an engineering-level-accurate database for the global vehicle forces and moments. Appropriate assumptions were made to provide for computational efficiency. The impact of these assumptions was examined through comparisons between ground-test data and predictions, as well as comparisons between various computations (such as inviscid and viscous solutions). Although the methods described here have been deemed sufficient to resolve global forces and moments, localized quantities are not necessarily fully resolved everywhere.

Analysis Tools

The primary CFD tool used for the preflight performance analysis of the X-43A is the GASP.[3] GASP is a multiblock, structured-grid, upwind-based, Navier–Stokes flow solver. Mixtures of thermally perfect gases are modeled using polynomial curve fits for thermodynamic properties.[4] GASP can model frozen, equilibrium, or finite-rate chemistry with models for hydrogen–air combustion. The Baldwin–Lomax algebraic turbulence model with the Goldberg backflow correction has been widely applied for turbulent flows.[5] Various two-equation eddy-viscosity formulations are also available in GASP and have been used for various applications. Convergence acceleration options include a V-cycle multigrid algorithm, mesh sequencing and local time stepping. A large calibration database is available for GASP for hypersonic configurations and scramjet flowfields. Predictions for surface pressure, flowfield quantities, and integrated forces and moments have compared well to available experimental data at unpowered and simulated powered conditions in previous studies.[6–11]

Two additional tools are used for analysis of the internal propulsion flowpath. The first is the supersonic hydrogen injection program (SHIP).[12,13] SHIP uses the SIMPLE method to solve the parabolized, mass-averaged equations for conservation of mass, momentum, total energy, total fuel, and turbulence fields in a variable area domain of rectangular cross section. The second tool used for flowpath analysis is the SRGULL code. SRGULL comprises a two-dimensional/axisymmetric Euler flow solver (SEAGULL),[14] which is used to solve the forebody, inlet, and external nozzle regions of the lower surface flowpath, and a one-dimensional chemical equilibrium cycle analysis code (SCRAM),[15] which is used to approximate the combustor flowfield. SRGULL also includes an integral boundary-layer method (HUD)[16,17] to provide a viscous component to the forces and moments and has a one-dimensional isolator model used to predict the onset location of pressure rise ahead of the fuel injectors associated with heat addition due to combustion. Several scaling factors, based on previous studies and ground-test data, are included to account for such factors as mass spillage, inlet kinetic energy efficiency, base pressure, combustion efficiency, and nozzle thrust multiplier to account for three-dimensional effects.

Preflight Analysis Methodology

Figure 3 shows a summary of the analysis methodology for the X-43A vehicle. The development of the preflight aeropropulsive performance database includes an analysis of the postseparation point through the powered flight experiment. Although not the focus of this paper, the database also supports the ascent, stage separation, and postexperiment descent phases of the mission as well.[2] Three mission points are analyzed: cowl-closed, cowl-open unpowered, and cowl-open powered. Force and moment data for the cowl-closed configuration, obtained primarily in the NASA Langley Research Center 20-in. Mach 6 and 31-in. Mach 10 wind tunnels, comprised the baseline values for the aerodynamics database. After relevant corrections to the wind-tunnel data (blade interference, base pressurization, flow angularity), Mach 7 predictions were obtained by linearly interpolating between the Mach 7 and Mach 10 points.[18] Comparisons with wind-tunnel force and moment data are used to provide code calibration. Because of model scale and facility limitations, it is not possible to simulate the flow-through engine or to model powered effects in available aerothermodynamic facilities. CFD predictions, developed from GASP inviscid and SRGULL calculations, were used to determine the inlet-open and power-on performance increments. These increments were then applied to the experimental database to develop predictions for longitudinal performance for the cowl-open configuration. Viscous predictions for the cowl-closed configuration and a viscous tip-to-tail powered simulation at the target flight-test point are used to provide additional code calibration and assess the methodology used to build the database performance increments. Data are also available from tests of the Hyper-X Flight Engine/vehicle flowpath simulator (HXFE/VFS) in the NASA Langley Research Center 8-Foot High Temperature Tunnel (8-ft HTT).[19] The VFS is a full-scale model that duplicates the flowpath and chine surfaces of the X-43A but does not model other components, such as wings and tails. The VFS model mounted in the test section is shown in Fig. 4. The primary objective of these tests was to verify the propulsion thrust performance, fuel sequencing, and operability of all engine-related subsystems. Force and moment data for each of the three postseparation mission points (cowl-closed, cowl-open unpowered and cowl-open powered) near the scramjet test point were also obtained along with surface pressure data along the scramjet flowpath. The VFS configuration models all of the salient features of the flowpath surface affected by these transitions, including three-dimensional expansion of the scramjet exhaust plume over the aftbody surface. These data provide verification of the predicted force and moment increments as well as comparisons with pressure predictions along the flowpath surface to assess the methodology.

The inlet-open and power-on longitudinal performance increments were computed using GASP to obtain three-dimensional inviscid flow solutions for the X-43A airframe and SRGULL computations for the propulsive flowpath surfaces of cowl-open configurations from the cowl leading-edge station to the vehicle trailing

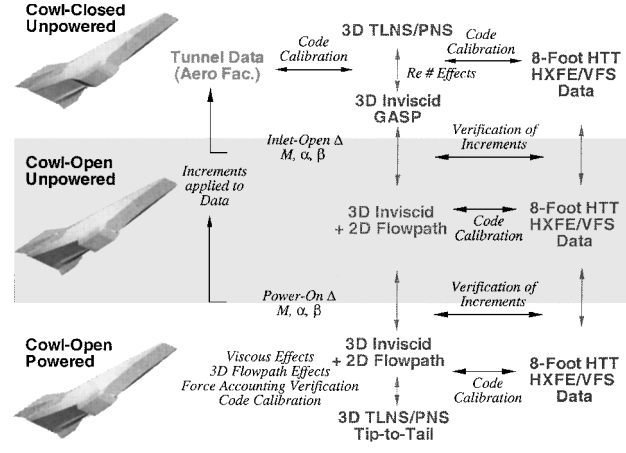

Fig. 3 Integrated aeropropulsive CFD methodology.

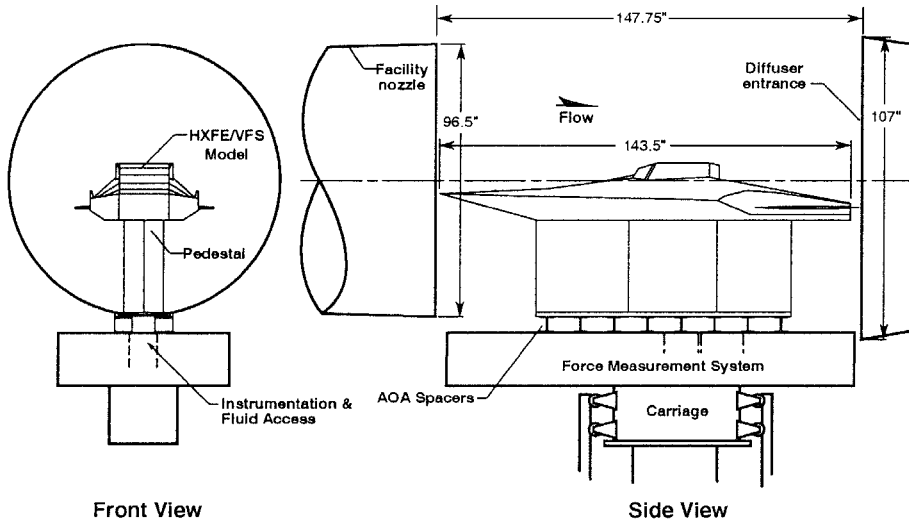

Fig. 4 HXFE/VFS model installed in the 8-ft HTT.

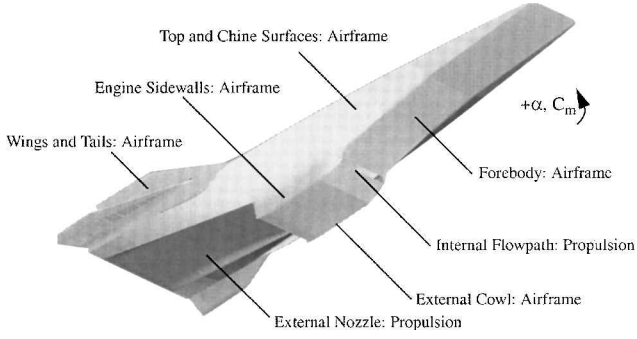

Fig. 5 X-43A force accounting methodology.

edge (inlet/isolator, combustor, and internal and external nozzle). Figure 5 shows the force accounting system used in this methodology. Internal flowpath surfaces, from cowl leading edge to cowl trailing edge, are accounted for as propulsion surfaces, and forces and moments are obtained from the SRGULL computations. The inviscid analysis in SRGULL assumes a sharp cowl leading edge. The effect of this assumption was evaluated through a viscous tip-to-tail calculation performed at the target flight-test point. Comparisons between SRGULL and viscous CFD predictions show that although shock impingement locations are affected inside the inlet and isolator, force and moment contributions from the internal flowpath surfaces are not significantly different. The external nozzle surface contribution is also obtained from SRGULL. All other external surfaces are accounted for as airframe surfaces, and force and moment contributions are obtained from the GASP calculations. This accounting system was selected to utilize the strengths of available analysis tools, allowing parametrics to be run with engineering cycle codes. Because interactions between propulsion and aerodynamic flowfields may impact aerodynamic forces and moments, trim characteristics, and overall vehicle performance, the separation of aftbody forces as shown in Fig. 4 assumes minimal spillage of the exhaust plume on to the airframe surfaces. The viscous tip-to-tail calculation at powered conditions can be used to examine characteristics of the exhaust plume and the effects of propulsion–airframe interactions on integrated forces and moments. The vehicle blunt base was not included in the three-dimensional CFD calculations. The effect of the blunt base is captured in the wind-tunnel measurements for the cowl-closed configuration with the CFD predictions used to compute the increments for the cowl-open performance. Therefore, the effects of the powered exhaust plume on the vehicle base are not captured in the analysis. The magnitude of the change in base force due to Reynolds number effects was assessed with two-dimensional calculations of the vehicle nozzle and blunt base. These computations enabled an assessment of uncertainty due to Reynolds number differences from ground to flight.

The inviscid calculations were obtained using a space-marching technique with the exception of the blunt nose of the vehicle. Sidewall, cowl, and wing leading edges are treated as aerodynamically sharp. The use of the inviscid approximation significantly reduces computational time and allows multiple parametrics to be analyzed. Solutions were obtained for the flight-scale X-43A over a matrix of points that included variations of Mach number and angle of attack around the Mach 7, 2-deg angle-of-attack flight-test point. Convergence is judged by examining surface pressure values and integrated forces and moment. A reduction of four orders of magnitude in the $L2$ norm of the residual vector is sufficient to achieve iteration convergence. The inviscid predictions for the cowl-closed configuration were obtained by fairing over a portion of the external nozzle to eliminate the requirement to solve the separated flow region behind the nozzle exit plane. Comparisons with viscous computations that solve this separated flow region were used to assess the impact of this geometry assumption on global forces and moments.

Viscous predictions of the cowl-closed configuration were obtained at various conditions to examine trends due to Reynolds number effects. The GASP calculations are performed by space marching over most of the body, with the exception of the blunt nose region and the wake region aft of the cowl trailing edge in the aftbody. The Baldwin–Lomax algebraic model is used as the turbulence model in these calculations with the transition location fixed based on estimations of the effectiveness of boundary-layer transition strips on the forebody (see Ref. 20). Previous experience has shown that this model is adequate for the prediction of flowfield and surface quantities, particularly skin friction, for external aerodynamic flows. Solution convergence is judged by examining integrated pressure and shear forces. A series of parabolized Navier–Stokes (PNS) forebody calculations were also used to calculate inlet mass capture, determine inlet entrance-plane flow profiles, examine boundary-layer properties, and calibrate pressure measurements for a flush-air data sensor (FADS) system.

A viscous tip-to-tail calculation, including a simulation of powered effects, was used to provide the most detailed prediction of performance at the target flight-test point of Mach 7, 2-deg angle of attack.[21] This calculation was accomplished using GASP to simulate both external and internal flowfields, including modeling the powered scramjet exhaust effects. A one-dimensional cycle analysis from SRGULL was still used to approximate the combustor flowfield due to the complexity of modeling the geometry of this region as well as the physical modeling requirements and computational cost to compute turbulent reacting flowfields in the combustor. A summary of the tip-to-tail methodology is shown in Fig. 6. External flowfields were computed by solving the PNS equations except in the regions of the nose and cowl leading edge, where bluntness effects are important. The scramjet exhaust plume is modeled as a single-species thermally perfect gas.

Code Calibration and Accuracy Assessment

Code calibration and accuracy assessment is accomplished, in part, through appropriate comparisons of CFD predictions with available experimental data. Figure 7 shows a comparison of force and moment predictions from three-dimensional GASP inviscid and viscous computations of the X-43A cowl-closed configuration with subscale wind-tunnel data at Mach 6. The results from a viscous computation shown in the Fig. 7 were obtained at the same Reynolds number and model scale as the data. There is an obvious discrepancy with the inviscid CFD axial force prediction. The agreement is much better for the viscous computation. Normal force coefficient is also slightly overpredicted, and somewhat smaller nose-up pitching moment values are predicted than are indicated by the database comparisons. There is little significant difference between the inviscid and viscous computations in normal force or pitching moment at 0-deg angle of attack. The discrepancy in pitching moment corresponds to a difference of less than 1 deg of elevator deflection required for trim at these conditions. This small discrepancy may be the result of several factors, including corrections made to the data and modeling approximations in the calculations. The data shown in Fig. 7 have been corrected for sting interference effects, base pressurization, and other facility and testing procedure effects. Inviscid surface pressure predictions do not differ substantially from viscous predictions for external airframe surfaces, suggesting that the inviscid approximation is sufficient to obtain accurate pressure loads on these surfaces. This comparison also shows that the assumption made to fair over a portion of the external nozzle surface for the inviscid marching calculations does not significantly affect global vehicle forces and moments. Surface pressure comparisons between viscous and inviscid cowl-closed calculations show that pressures are only affected in the immediate vicinity of the internal nozzle exit plane. Variations in freestream Reynolds number and model scales affect only the skin-friction contribution to total axial force.

Forebody pressure data are available at a few discrete locations for a 0.8-scale forebody model used to calibrate FADS instrumentation in wind-tunnel testing. Figure 8 shows this comparison at a forebody cross section location of $x = 24.0$ in. from the nose at Mach 6 freestream conditions over an angle-of-attack range from -2 to 8 deg. Pressure taps are present on the centerline on both the upper and lower surfaces, as well as near the outer edge of the forebody chine surfaces. This forebody station is downstream of the boundary-layer trip location and upstream of the compression

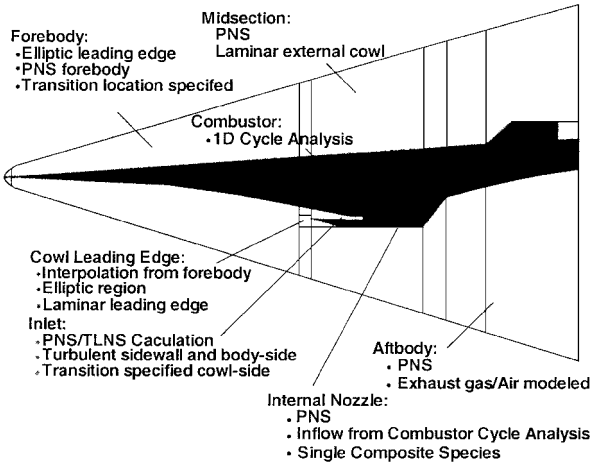

Fig. 6 Three-dimensional tip-to-tail solution methodology.

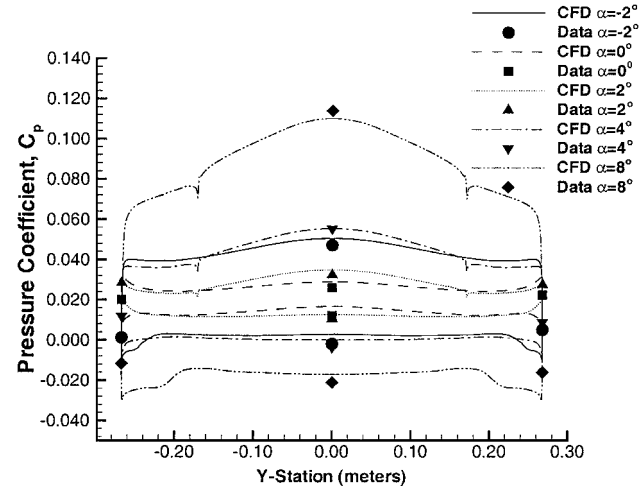

Fig. 8 Comparisons of wind-tunnel surface pressure measurements and CFD predictions at the x = 24.0 in. forebody station.

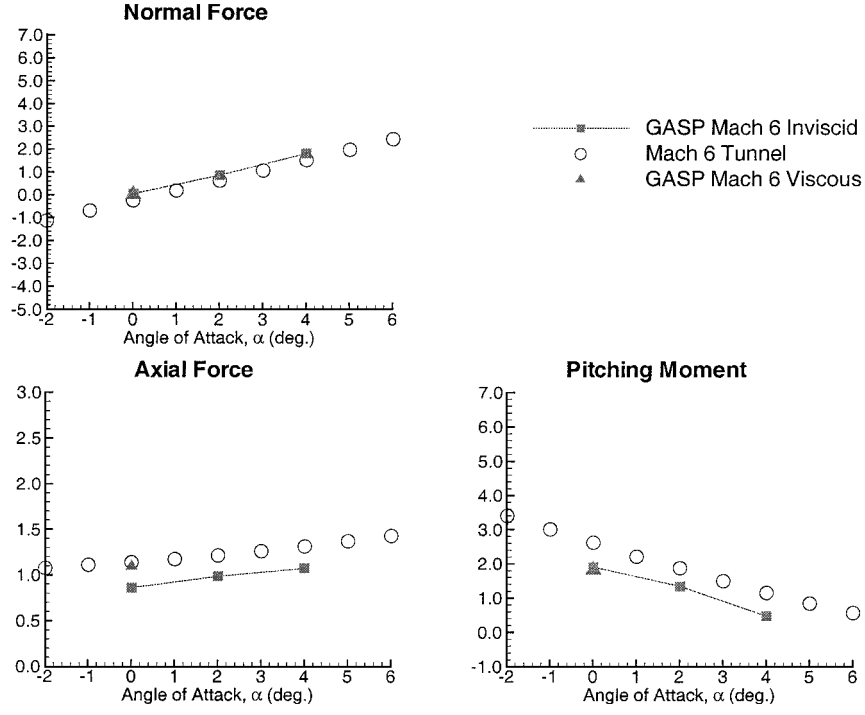

Fig. 7 X-43A normalized cowl-closed predictions vs subscale experimental database at Mach 6.

ramp break located at the $x = 37.3$-in. station. The CFD predictions show good agreement with data at the centerline locations. The outer-edge predictions are difficult to compare because the pressure rapidly changes around the leading edge.

Verification of predicted force and moment coefficients from SRGULL is accomplished primarily through comparisons of SRGULL surface pressure and force and moment predictions with higher-fidelity CFD solutions for comparable component efficiencies, as well as appropriate comparisons between predictions and data. Experimental measurements from various scramjet flowpath tests in NASA Langley Research Center scramjet test facilities have shown good agreement in terms of axial force and surface pressure predictions. Surface pressure comparisons in the inlet/isolator and nozzle regions show good agreement with shock locations and pressure levels. Correlations of pitching moment have also been obtained.

Comparisons of surface pressure predictions have been made with data from the 8-ft HTT tests of the HXFE/VFS model. The 8-ft HTT is a propulsion test facility that uses methane–air combustion and oxygen replenishment to generate a test gas with a total enthalpy and a Mach number equivalent to flight conditions.[22] Therefore, the oxygen content of the freestream gas is representative of flight conditions as is the Mach number, total enthalpy, dynamic pressure, and Reynolds number. In general, comparisons of external forebody and aftbody pressure predictions from the SRGULL and inviscid GASP solutions used in the database buildup at both powered and unpowered conditions show good agreement with the HXFE/VFS data. Figure 9 shows a comparison of normalized forebody surface pressure predictions with HXFE/VFS data along the model centerline. Predictions from both GASP and SRGULL calculations are shown in Fig. 9. Comparisons of internal engine surface pressure predictions from SRGULL also show reasonable agreement with HXFE pressure data, although higher-fidelity Navier–Stokes solutions are required to resolve fully the details of the scramjet flowfield. The pressure data comparisons also suggest that testing in the vitiated-air environment of the 8-ft HTT provides a reasonable simulation of aerodynamic force and moment increments at the Mach 7 target flight conditions.

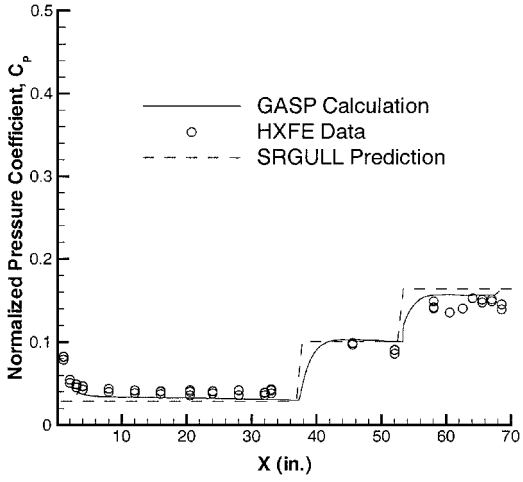

Fig. 9 Normalized forebody surface pressure predictions with comparisons to HXFE measurements.

Experimental verification of the CFD-computed longitudinal force and moment database predictions for the cowl-open configurations was obtained from the HXFE/VFS tests. Because of the differences in geometry, only the force and moment increments for the cowl-open and power-on sequences obtained in the test can be utilized. Figure 10 shows a comparison of lift, drag, and pitching moment coefficient at Mach 7 computed by applying both the database increments and the measured HXFE increments to the cowl-closed database values. The uncertainty estimates in Fig. 10 correspond to 3-sigma deviations from the time-averaged values shown for the experimental data. In general, the measured increments show excellent agreement with the predictions. The magnitude of axial and normal force as well as the pitching moment increments are comparable, and the measurements confirm a nose-down pitching moment resulting from the cowl-opening sequence and the power-on sequence.

Finally, an analysis of aftbody flowfield features from the viscous tip-to-tail calculation reveals some characteristics of the scramjet exhaust plume and the impact of plume expansion on force and moment accounting. Figure 11 shows density contours of the exhaust plume species at several cross sections along the aftbody. Figure 11 indicates that the plume expands beyond the propulsion surface as defined in the force accounting system shown in Fig. 5 and impinges

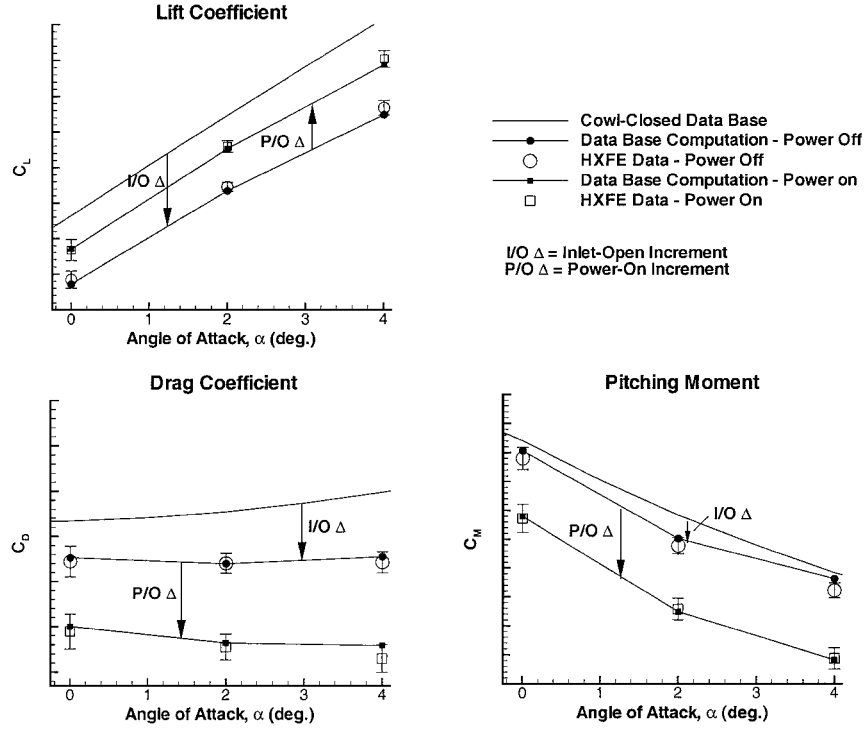

Fig. 10 Normalized force and moment database predictions with comparisons to HXFE measured increments.

on the airframe surfaces, although there is no interaction with the wing surface. A comparison of total integrated forces and moments from this calculation with those developed from the database build up methodology shows only small differences in predicted axial force and pitching moment, indicating that this spillage effect is small at the nominal Hyper-X scramjet flight-test condition. The effects of plume–airframe interaction at higher angles of attack, off-nominal engine operating conditions, or with control-surface deflections remain an issue for airframe-integrated scramjet-powered configurations. Also note that this force accounting system is specific to the X-43A vehicle. The X-43A was a point-design configuration, and analysis has focused on a narrow window of flight-test conditions. Future hypersonic vehicle concepts designed to function over a broader range of operating conditions will require appropriate force accounting systems and methods to evaluate fully these propulsion–airframe integration issues.

Lateral-Directional Stability Characteristics

No experimental force and moment data are available for the cowl-open configurations at nonzero sideslip angles. The assumption was made in initial X-43A database releases that lateral-directional stability characteristics do not change significantly due to the cowl-opening and power-on mission sequences and that the cowl-closed experimental data can be used to model these effects at the other mission points. To verify this assumption, computations were obtained on the X-43A for the cowl-closed and cowl-open configurations.[23] Three-dimensional inviscid computations were obtained at Mach 7, 2-deg angle of attack, and 0-deg and 3-deg sideslip. Both unpowered and powered conditions were analyzed for the cowl-open configuration. The unpowered computations were obtained using GASP, including the internal flowpath without the geometry of the fuel injectors in the combustor. The powered computations were obtained using GASP and the one-dimensional cycle analysis method in SRGULL for the combustor. Three lateral stations were computed for the combustor analysis to approximate the lateral variation in flowfield properties at the 3-deg sideslip condition. Figure 12 shows predicted values for side force, yawing moment, and rolling moment derivatives computed from the 0-deg and 3-deg predictions at Mach 7. The cowl-closed experimental database values are also shown in Fig. 12 for comparison. Although some differences exist between the database values and the CFD predictions, the significance is in the comparison among the three CFD calculations. The differences in the predicted stability derivatives are negligible. Therefore, the analysis predicts that the cowl-opening and power-on sequences of the flight have little significant direct effect on the lateral-directional stability. There is, however, a significant indirect effect of the powered flight condition at sideslip on airframe stability and control as a result of the horizontal wing deflection required to trim the resultant propulsive-induced pitching moment. An analysis of the aftbody flowfield solution also indicates some impingement of the powered scramjet exhaust plume on the leeward-side horizontal wing surface of the vehicle at the 3-deg sideslip, 2-deg angle-of-attack condition. No analysis was done to evaluate control surface effectiveness under powered conditions or to evaluate exhaust plume interaction effects at nonzero sideslip with deflected wing surfaces.

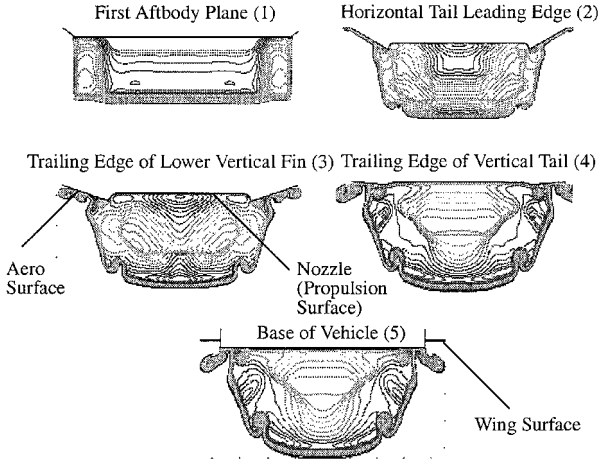

Fig. 11 Density contours showing three-dimensional exhaust plume expansion.

Conclusions

CFD and other analytical tools have been used in the development and preflight analysis of the Mach 7 X-43A vehicle. Integrated aeropropulsive performance was predicted using three-dimensional inviscid airframe computations and engineering cycle analysis results. Viscous tip-to-tail calculations for the cowl-closed configuration

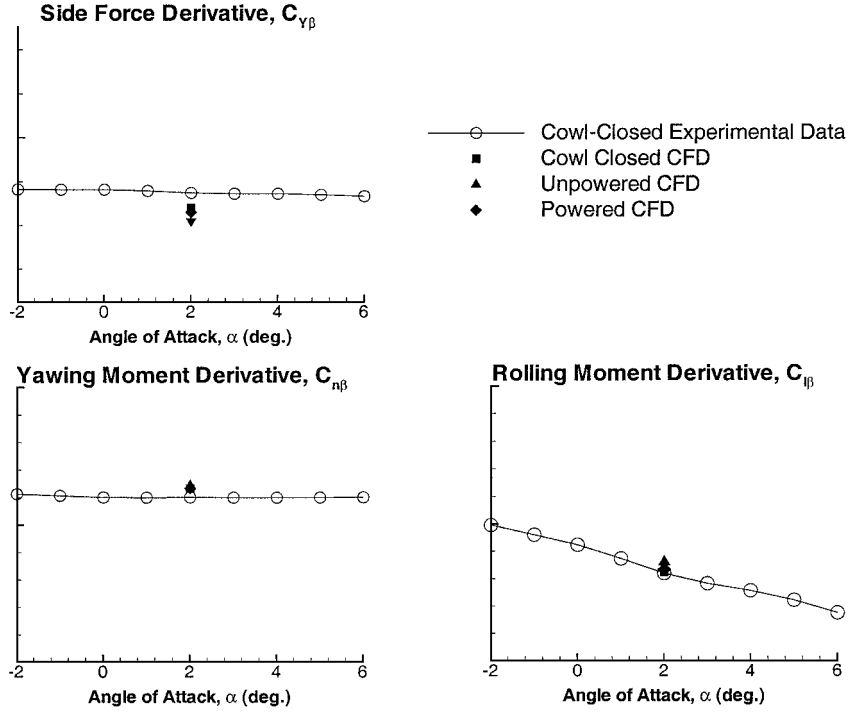

Fig. 12 Inviscid CFD predictions of X-43A lateral-directional stability derivatives at Mach 7.

and the powered cowl-open configuration at the target Hyper-X flight-test point were used to provide detailed performance information and assessment of the database prediction methodology. Integrated force and moment predictions from inviscid and viscous cowl-closed calculations show good agreement with available wind-tunnel data. Longitudinal performance increments compare well with measured increments from integrated flowpath tests of the HXFE. Surface pressure predictions also compare well with limited wind-tunnel data and HXFE flowpath data. CFD was also used to assess qualitatively lateral-directional stability characteristics and predict that the cowl-opening and power-on sequences have no significant direct effect on lateral-directional stability characteristics. The Mach 7 X-43A flight test will provide the first-ever flight data for an airframe-integrated scramjet-powered configuration. An assessment of these data with comparisons to ground-test data and predictions will provide for an assessment of analysis techniques, predictive assumptions and ground-to-flight scaling of performance data.

References

[1]Freeman, D. C., Jr., Reubush, D. E., McClinton, C. R., Rausch, V. J., and Crawford, J. L., "The NASA Hyper-X Program" 48th International Astronautical Conf., Turin, Italy, Oct. 1997.

[2]Engelund, W. C., Holland, S. D., Cockrell, C. E., Jr., and Bittner, R. D., "Aerodynamic Database Development for the Hyper-X Airframe Integrated Scramjet Propulsion Experiments," *Journal of Spacecraft and Rockets*, Vol. 38, No. 6, 2001, pp. 803–810.

[3]Godfrey, A. G., "General Aerodynamic Simulation Program Version 3.0 User's Manual," Aerosoft, Inc., Blacksburg, VA, May 1996.

[4]Svehle, R. A., and McBride, B. J., "Fortran IV Computer Program for Calculation of Thermodynamic and Transport Properties of Complex Chemical Systems," NASA TN D-7056, 1973.

[5]Goldberg, U. C., "Separated Flow Treatment with a New Turbulence Model," *AIAA Journal*, Vol. 24, No. 10, 1986, pp. 1711–1713.

[6]Huebner, L. D., and Tatum, K. E., "Computational and Experimental Aftbody Flowfields for Hypersonic Airbreathing Configurations with Scramjet Exhaust Flows," AIAA Paper 91-1709, June 1991.

[7]Huebner, L. D., and Tatum, K. E., "CFD Code Calibration and Inlet-Fairing Effects on a Three-Dimensional Hypersonic Powered-Simulation Model," AIAA Paper 93-3041, July 1993.

[8]Tatum, K. E., Witte, D. W., Monta, W. J., and Walters, R. W., "Analysis of Generic Scramjet External Nozzle Flowfields Employing Simulant Gases," AIAA Paper 90-5242, Dec. 1990.

[9]Srinivasan, S., Bittner, R. D., and Bobskill, G. J., "Summary of the GASP Code Application and Evaluation Effort for Scramjet Combustor Flowfields," AIAA Paper 93-1973, June 1993.

[10]Loomis, M. P., Venkatapathy, E., Papadopoulos, P., Davies, C. B., Berry, S., Horvath, T., and Campbell, C., "Aeroheating and Aerodynamic CFD Validation and Prediction for the X-38 Program," AIAA Paper 97-2478, June 1997.

[11]Hollis, B., Horvath, T. J., Berry, S. A., Hamilton, H., and Alter, S., "X-33 Computational Aeroheating Predictions and Comparisons with Experimental Data," AIAA Paper 99-3559, July 1999.

[12]Markotos, N. C., Spalding, D. B., and Tatchell, D. G., "Combustion of Hydrogen Injected into a Supersonic Airstream (The SHIP Computer Program)," NASA CR-2802, April 1977.

[13]Ferlemann, P. G., "Improvements to the SHIP Computer Code and Predictions of Vorticity Enhanced Turbulent Supersonic Mixing," M.S. Thesis, School of Engineering and Applied Science, George Washington Univ., Washington, DC, Aug. 1993.

[14]Salas, M. D., "Shock Fitting Method for Complicated Two-Dimensional Supersonic Flows," *Proceedings of the AIAA 2nd Computational Fluid Dynamics Conference*, AIAA, New York, 1975.

[15]Pinckney, S. Z., "Internal Performance Predictions for Langley Scramjet Engine Module," NASA TM X-74038, Jan. 1978.

[16]Pinckney, S. Z., "Turbulent Heat-Transfer Prediction Method for Scramjet Engines," NASA TN D-7810, Nov. 1974.

[17]Pinckney, S. Z., "Method for Predicting Compressible Turbulent Boundary Layers in Adverse Pressure Gradients," NASA TM X-2302, Aug. 1971.

[18]Holland, S. D., Woods, W. C., and Engelund, W. C., "Hyper-X Research Vehicle Experimental Aerodynamics Test Program Overview," *Journal of Spacecraft and Rockets*, Vol. 38, No. 6, 2001, pp. 828–835.

[19]Huebner, L. D., Rock, K. E., Witte, D. W., Ruf, E. G., and Andrews, E. H., Jr., "Hyper-X Engine Testing in the NASA Langley 8-Foot High Temperature Tunnel," AIAA Paper 2000-3605, July 2000.

[20]Berry, S. A., Auslender, A. H., Dilley, A. D., and Calleja, J. F., "Hypersonic Boundary-Layer Trip Development for Hyper-X," *Journal of Spacecraft and Rockets*, Vol. 38, No. 6, 2001, pp. 853–864.

[21]McClinton, C. R., Voland, R. T., Holland, S. D., Engelund, W. C., White, J. T., and Pahle, J. W., "Wind Tunnel Testing, Flight Scaling and Flight Validation with Hyper-X," AIAA Paper 98-2866, June 1998.

[22]Huebner, L. D., Rock, K. E., Voland, R. T., and Wieting, A. R., "Calibration of the Langley 8-Foot High Temperature Tunnel for Hypersonic Propulsion Airbreathing Testing," AIAA Paper 96-2197, June 1996.

[23]Frendi, A., "On the CFD Support for the Hyper-X Aerodynamic Database," AIAA Paper 99-0885, Jan. 1999.

W. E. Williamson
Associate Editor